Analysis of ATCA Radio Continuum Data towards Imaging a Radio Galaxy

A REPORT

submitted in requirement of Visiting Student Program

by

Deepak Kumar Deo

(VSP Student)

under the supervision of

Dr. Lakshmi Saripalli

&

Dr. Ravi Subrahmanyan

Department of Astronomy and Astrophysics
Raman Research Institute, Bangalore

March 13, 2015

Acknowledgement

I would like to thank Dr. Lakshmi Saripalli and Dr. Ravi Subrahmanyan for being very supportive supervisors. I am extremely grateful to Dr. Lakshmi for constantly motivating me and making me believe in myself, besides being a supportive supervisor she was also a good teacher to me, her way of explaining and connecting one thing from other was simply the perfect, she taught me to get the feel of the subject and appreciate it. I also wish to express my sincere gratitude towards Dr. Ravi whose computational expertise, very clear and simple explanation helped me to go through my data analysis work smoothly. I am extremely thankful to both of my supervisors for their invaluable time, patience and guidance without which this wouldn't have been possible.

I would also like to thank my friend Sree Vani for the insightful discussions I had with her which helped in smooth progress of my work. Despite being busy in her own project she was always ready to discuss with me and clear even silliest of my doubts, am thankful to her for being with me throughout the project.

I am also thankful to office staffs of Raman Research Institute especially Vidya ma'am for providing me with office space and also the canteen staffs for delicious lunch.

Finally, I would like to thank my parents for being patient, supportive and encouraging towards pursuit of my dreams and raising me as a good person.

Deepak Kumar Deo

List of Figures

Abbreviations

FR	**F**anaroff **R**iley
ATLBS	**A**ustralia **T**elescope **L**ow, **B**rightness **S**urvey
MIRIAD	**M**ultichannel **I**mage **R**econstruction, **I**mage **A**nalysis and **D**isplay
CASA	**C**ommon **A**stronomy **S**oftware **A**pplications
CABB	**C**ompact **A**rray **B**roadband **B**ackend
ATCA	**A**ustralia **T**elescope **C**ompact **A**rray
RPFITS	**R**adio**P**hysics **F**lexible **I**mage, **T**ransport **S**ystem
RFI	**R**adio **F**requency **I**nterference
FITS	**F**lexible **I**mage, **T**ransport **S**ystem
MS	**M**easurement **S**et
NRAO	**N**ational **R**adio, **A**stronomy **O**bservatory
FT	**F**ourier **T**ransformation
PSF	**P**oint **S**pread **F**unction

Contents

1 Introduction

On the basis of morphologies radio galaxies have been classified as FR-I and FR-II and the object we are analysing is a large FR-II radio galaxy spread over ≈ 17 arc minutes in North-South direction as can be seen in Fig 1.2 (Right). Our target source is a FR-II radio galaxy from ATLBS[1] which among the imaged has the lowest surface brightness lobes known to date. Fig 1.1 shows the complete ATLBS image showing our target source in a rectangular box. This source has been imaged at 1.4 GHz previously (Saripalli et al, 2012[2]) and has been classified as FR-II (restarted) type. Restarted sources are thought to have undergone a new activity episode after a period over which the nuclear activity had stopped. In this source the presence of edge brightened lobes without compact hotspots at their ends and instead only an edge brightened but recessed feature in the northern lobe indicates the restarted nature. To derive the spectral indices over a broader range of frequencies than available the source was observed once again.

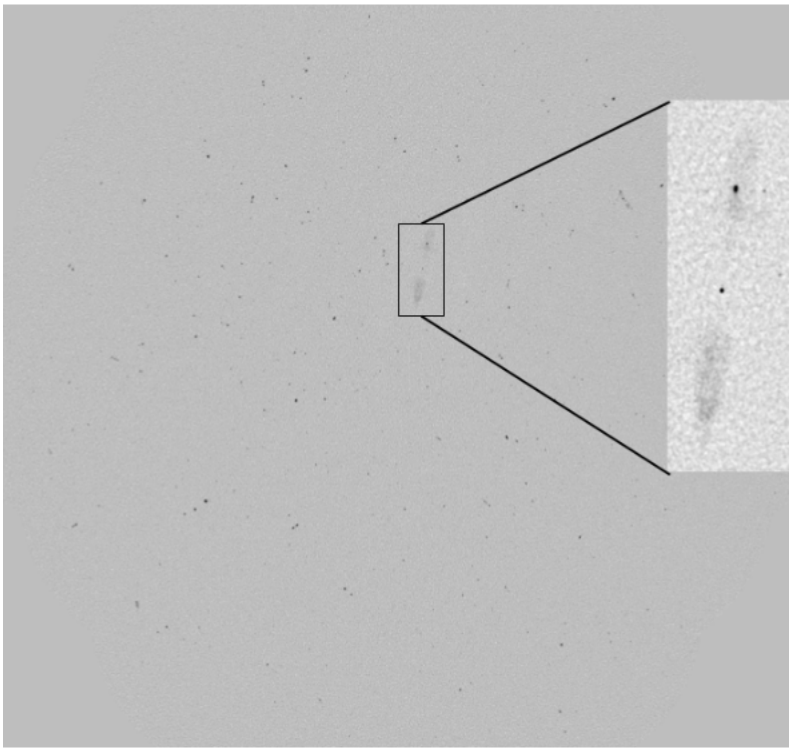

Figure 1.1: ATLBS image showing the target source in box

1.1 Observations

The new observations were carried out using ATCA[3] at two different higher frequencies 5.5GHz and 9GHz spread over a bandwidth of 2GHz consisting of 2049 channels each of 1MHz. Also since the source has large angular size, it was observed over 27 different pointings consisting of 3 RAs and 9 DECs, thus creating a mosaic. As the size of individual telescope dishes in ATCA is 22 m and therefore the primary beams[1] at 5.5GHz and 9GHz are respectively ≈ 8.5 and ≈ 5 arcmin, it wouldn't have been possible to cover a large source of 17 arcmin with such smaller beams adequately. Hence several pointings were used. Fig 1.2 (Left) depicts the phase center associated with each of the poinitings.

Pointings	RA	DEC
rg_1	00:34:28.85	-66:30:11.15
rg_2	00:34:28.85	-66:32:31.55
rg_3	00:34:28.85	-66:34:51.95
rg_4	00:34:28.85	-66:37:12.35
rg_5	00:34:28.85	-66:39:32.75
rg_6	00:34:28.85	-66:41:53.15
rg_7	00:34:28.85	-66:44:13.55
rg_8	00:34:28.85	-66:46:33.95
rg_9	00:34:28.85	-66:48:54.35
rg_10	00:34:05.23	-66:30:11.15
rg_11	00:34:05.23	-66:32:31.55
rg_12	00:34:05.23	-66:34:51.95
rg_13	00:34:05.23	-66:37:12.35
rg_14	00:34:05.23	-66:39:32.75
rg_15	00:34:05.23	-66:41:53.15
rg_16	00:34:05.23	-66:44:13.55
rg_17	00:34:05.23	-66:46:33.95
rg_18	00:34:05.23	-66:48:54.35
rg_19	00:33:41.61	-66:30:11.15
rg_20	00:33:41.61	-66:32:31.55
rg_21	00:33:41.61	-66:34:51.95
rg_22	00:33:41.61	-66:37:12.35
rg_23	00:33:41.61	-66:39:32.75
rg_24	00:33:41.61	-66:41:53.15
rg_25	00:33:41.61	-66:44:13.55
rg_26	00:33:41.61	-66:46:33.95
rg_27	00:33:41.61	-66:48:54.35

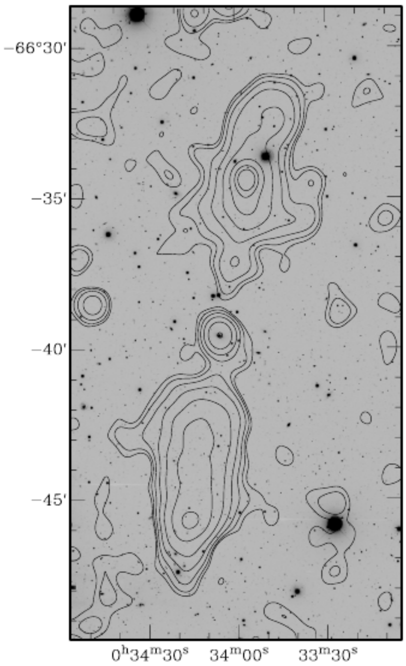

Figure 1.2: 27 pointings of mosaic (L) and source at 1.4GHz[2] (R)

Observations were taken by Dr. Ravi Subrahmanyan on 16th March 2014. It includes observing of a primary calibrator for ≈ 6 minutes at the beginning, a secondary calibrator for ≈ 3 minutes at regular intervals and all the different pointings of target source periodically over a span of ≈ 5 hours from 02:36 UTC to 07:10 UTC. The observed data is recorded in RPFITS format by ATCA which will undergo analysis through various steps, details about which and the calibrators have been discussed in data analysis section (2).

[1]Its the resolution of single dish telescope $= \frac{1.02\lambda}{D}$, D = Diameter of dish

2 | DATA Analysis

2.1 Introduction

Our data is a CABB[1] continuum dataset which comes from the ATCA experiment C2838 conducted on 16th March 2014. Recorded data-set will be analysed initially by MIRIAD[4] and then later by CASA[5]. Analysis involves following steps :

1. Loading the data
2. Calibration and Flagging
3. Applying Calibration
4. Data Reduction
5. Imaging and Deconvolution
6. Measurement

First three steps has to go through MIRIAD and the later three through CASA. This report consists of detail explanation of first four steps and a little about the fifth step. Analysis was carried over a span of three months from Dec., 2014 to Feb., 2015 and first four steps were carried out in this duration. Fifth and sixth steps required more involvement of time which I was short of.

2.2 MIRIAD Analysis

MIRIAD is a radio interferometry data-reduction package used for taking a raw visibility data through calibration to image analysis stage. Data can be a continuum or spectral line observations. Ours is a continuum uv data-set and its in RPFITS format which has to be converted into a MIRIAD readable format before being processed by it. Herein I have explained the tasks performed in MIRIAD details of which can also be found in MIRIAD cookbook[6].

[1]Its an upgrade to ATCA which increased ATCA's bandwidth from 128MHz to 2GHz

2.2.1 Loading the data

At first the recorded RPFITS uv data-set (2014-03-16_0235.C2838, 2014-03-16_0603.C2838) is loaded onto MIRIAD using task *atlod* in it. The parameters used for the task is as follows:

```
miriad% inp atlod
  Task: atlod
  in          = 2014-03-16_0235.C2838,2014-03-16_0603.C2838
  out         = C2838_2014-03-16.uv
  ifsel       =
  restfreq    =
  options     = birdie,rfiflag,noauto,xycorr
  nfiles      =
  nscans      =
  nopcorr     =
  edge        =
```

Inputs (*in*) are the visibilities in RPFITS and the output (*out*) in MIRIAD format. Besides converting *atlod* also performs some extra tasks which has been specified in options.

birdie - it is used for CABB data to delete 100 channels from the edges as those are unusable parts of spectrum caused due to the self-interference between the channels.

rfiflag - it flags the RFI i.e., those channels at which data is bad.

noauto - as we don't want autocorrelation data, hence we used it.(our source is orthogonally polarized in X and Y direction. XX,YY,XY and YX are the possible correlations).

xycorr - it is used to perform a phase correction between the X and Y products based on the online measurement of the XY phase.

To see the summary listing for data-set C2838_2014-03-16.uv we use task *uvindex*.

```
miriad% inp uvindex
  Task: uvindex
  vis          = C2838_2014-03-16.uv
  interval     =
  log          = C2838_2014-03-16.uv.log
  options      = mosaic
```

Our source was observed in a mosaic mode and to avoid the detailed information for different pointings of a mosaic in the log file, we have used the option 'mosaic' in task *uvindex*.

2.2.2 Splitting the data

From the log file C2838_2014-03-16.uv.log we observed that data-set consists of two different frequencies and hence we split it into separate frequency sets using the task *uvsplit*.

```
miriad% inp uvsplit
  Task: uvsplit
  vis          = C2838_2014-03-16.uv
  select       =
  options      = mosaic
  maxwidth     =
```

After running this task we see 6 different folders in our current working directory which are 1934-638.5500, 1934-638.9000, 2353-686.5500, 2353-686.9000, rg.5500 and rg.9000. 1934-638 is our bandpass and flux calibrator (primary calibrator), 2353-686 is our phase calibrator (secondary calibrator) and rg (radio galaxy) is the main source. 5500 and 9000 are the frequency (in MHz) at which our source and calibrators were observed.

2.2.3 Calibration and Flagging

We use 1934-638 for bandpass calibration because it is a bright point source and also for flux calibration because its flux density is known and is stable over time.

2353-686 is a point source nearby our main source and hence used for phase calibration. We start with primary calibrator to do bandpass and flux calibration and then we use it to calibrate secondary calibrator which is further used to calibrate our main source. Here we explain the whole calibration and further data analysis processes for 5.5 GHz which has been exactly followed for 9GHz too.

1934-638 was observed once for 6 minutes at the beginning of experiment. There was no need to observe it at periodic intervals as its flux density doesn't varies with time. Before any calibration and RFI flagging we can check how the amplitude varies with time (Fig 2.1) and with channel (Fig 2.2) for the primary calibrator using task *uvspec* and *uvplt* respectively.

```
miriad% inp uvspec
  Task: uvspec
  vis          = 1934-638.5550
  select       =
  line         =
  stokes       =
  interval     = 10
  hann         =
  offset       =
  options      =
  axis         = chan,amp
  yrange       =
  device       = /xs
  nxy          = 3,4
  log          =
```

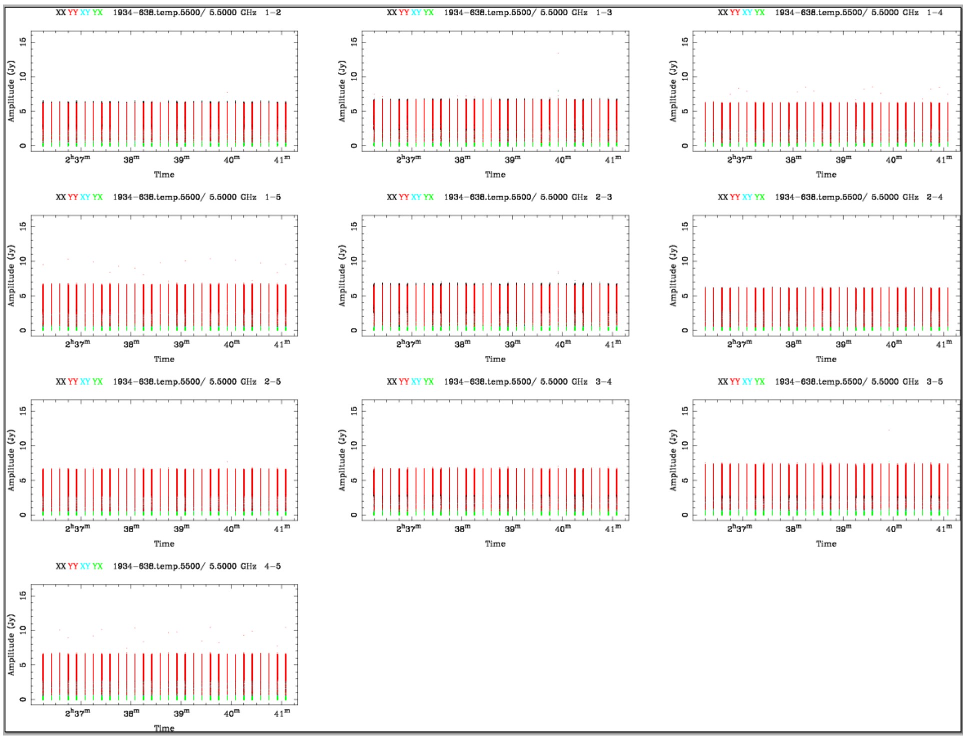

Figure 2.1: amplitude vs time before calibration and RFI flagging

```
miriad% inp uvplt
  Task: uvplt
  vis        = 1934-638.5500/
  line       =
  select     =
  stokes     =
  axis       = time,amp
  xrange     =
  yrange     =
  average    =
  hann       =
  inc        =
  options    = nofqav
  subtitle   =
  device     = /xs
  nxy        = 3,4
  size       =
  log        =
  comment    =
```

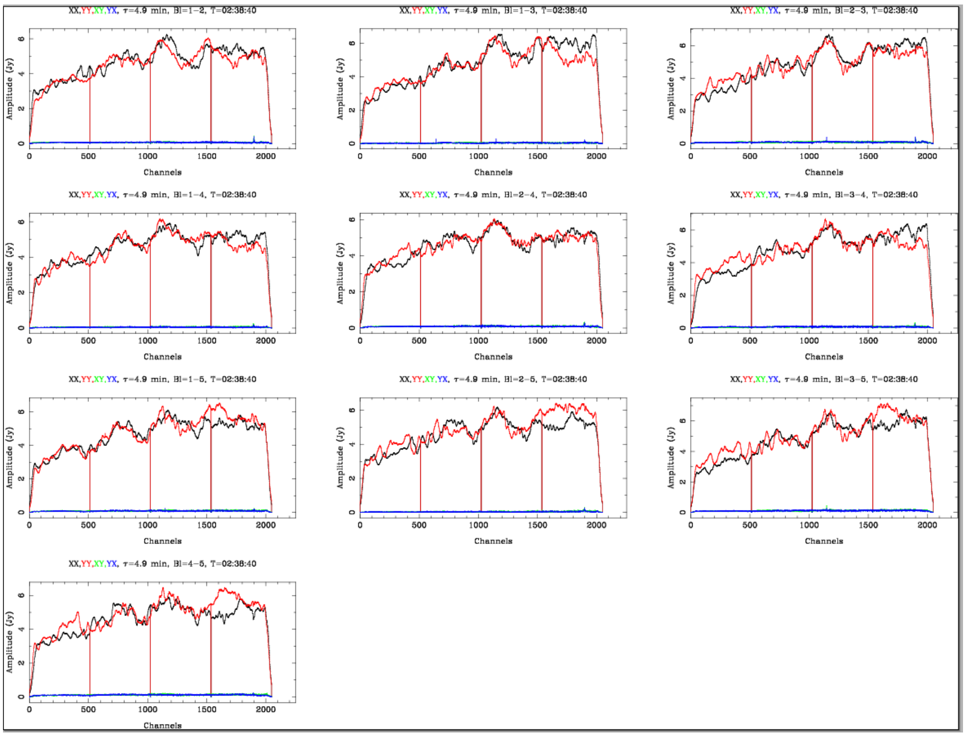

Figure 2.2: amplitude vs channel before calibration and RFI flagging

nofqav was used in option to disable the automatic averaging done over frequency by *uvplt*, as we want to observe the amplitude variation over whole bandwidth and not at a particular averaged frequency.

In the amplitude *vs* channel plot (2.2) the interference seen at the edges are due to self-interference within the channels and the peaks in between are due to external RFIs of which we get rid using the *birdie* and *rfiflag* options while performing task *atlod*. Fig 2.3 and Fig 2.4 shows the improvement in Fig 2.2 and Fig 2.1 after removing the bad data.

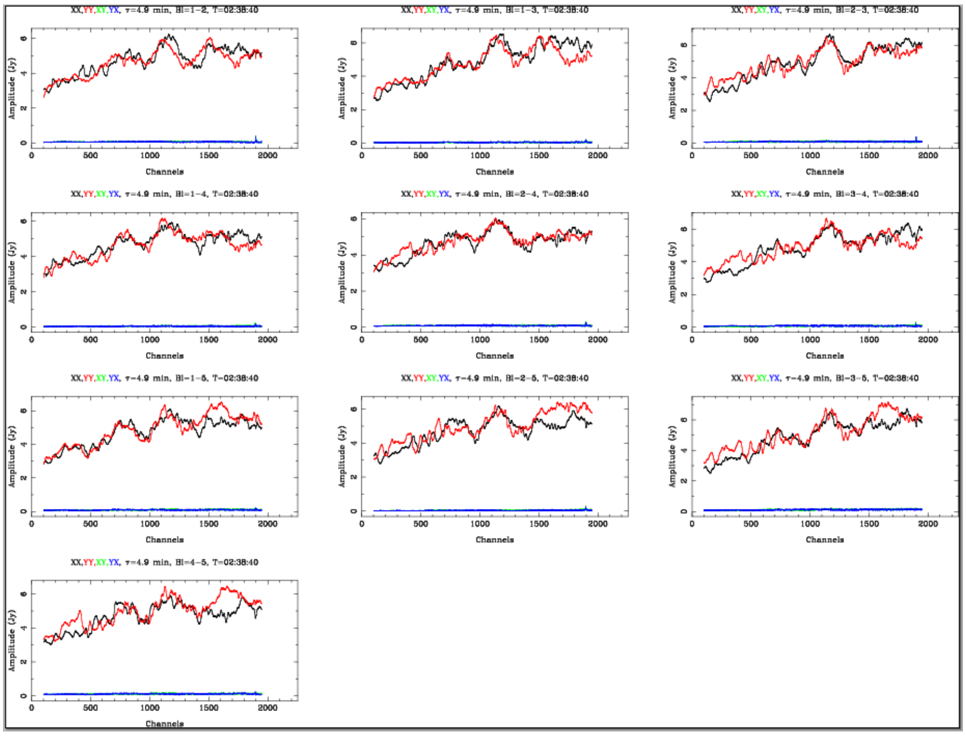

Figure 2.3: amplitude vs channel after RFI flagging

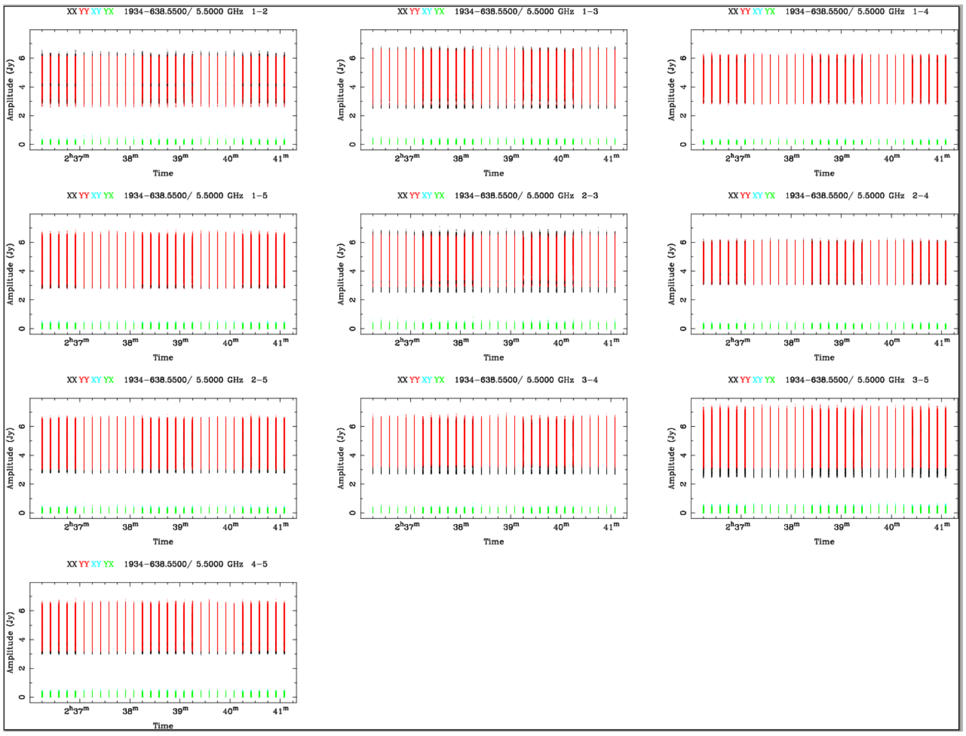

Figure 2.4: amplitude vs time after RFI flagging

From Fig 2.3 it follows that there are no RFI to flag and we can proceed towards calibration. If RFI would have been persisted even after *atlod* then they could be removed using any of the three flagging tasks : *uvflag*, *pgflag* or *blflag* details of which can be seen in cookbook[6]. We here use our primary calibrator 1934-638 as bandpass and flux calibrator and to determine bandpass solution we perform task *mfcal* on it for which syntax is as follows :

```
miriad% inp mfcal
  Task: mfcal
  vis        = 1934-638.5550
  line       =
  stokes     =
  edge       =
  select     =
  flux       =
  refant     =
  minants    =
  interval   =
  options    =
  tol        =
```

We then determine antenna gain solution and polarisation leakage solution by performing task *gpcal* on it.

```
miriad% inp gpcal
  Task: gpcal
  vis        = 1934-638.5500
  select     =
  line       =
  flux       =
  spec       =
  refant     =
  minants    =
  interval   = 0.1
  nfbin      = 4
  tol        =
  xyphase    =
  options    = xyvary
```

interval - it is in minutes and we use it small to determine the gain solution over short interval of time.
nfbin - it divides the whole bandwidth in assigned number of chunks, here it divides the ∼ 2GHz bandwidth in 4 equal chunks of 512MHz and determines the polarisation leakage solution for each chunks separately.
xyvary - it is used here to specify that XY phase varies with time which by default is taken as constant by *gpcal*.

Now at this point bandpass and flux calibration is complete and modification in Fig 2.3 and Fig 2.3 can be observed in Fig 2.5 and Fig 2.5.

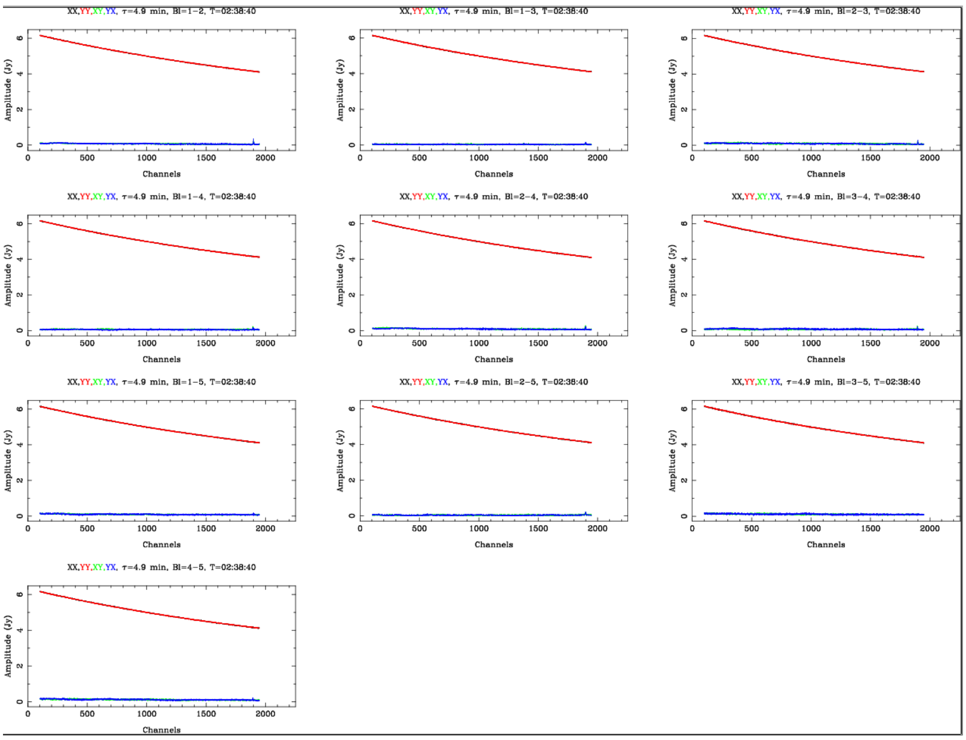

Figure 2.5: amplitude vs channel after bandpass and flux calibration

In Fig 2.6 the uniformity in amplitude over whole time depicts the good quality of calibration.

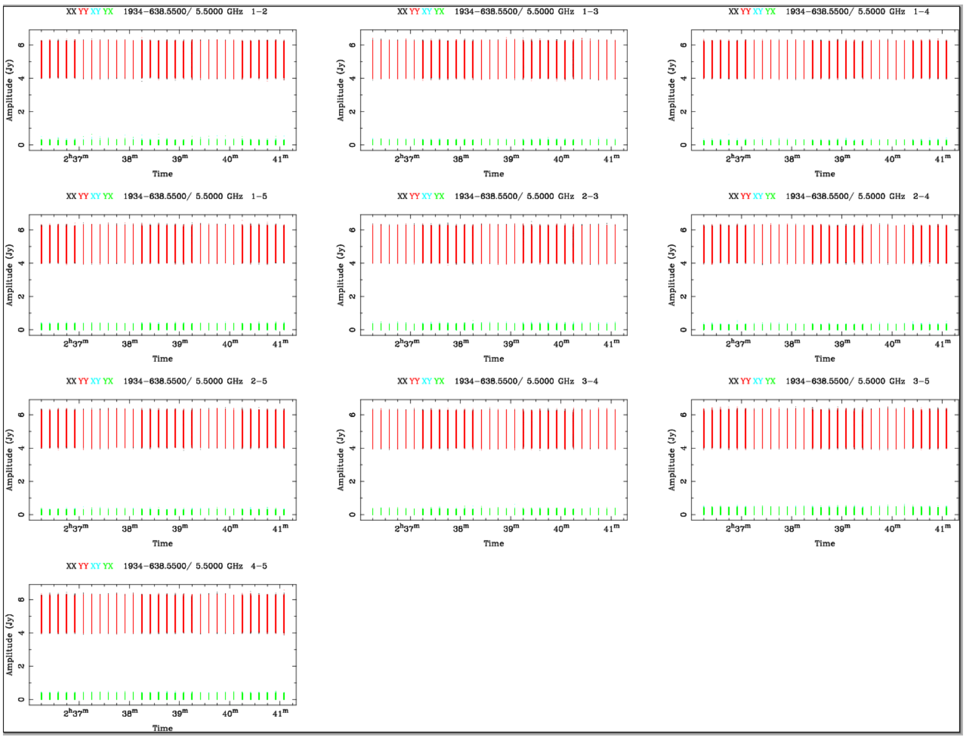

Figure 2.6: amplitude vs time after bandpass and flux calibration

We can also plot phase *vs* time to check the quality of calibration done on primary calibrator. On phase *vs* time plot we expect to see the phase around 0 degrees and in Fig 2.7 which is the plot for parallel correlations (*xx, yy*), we observe it around 0 degrees but in case of orthogonal correlations (xy, yx) (Fig 2.8) phase is varying from -150 to -150 degrees.

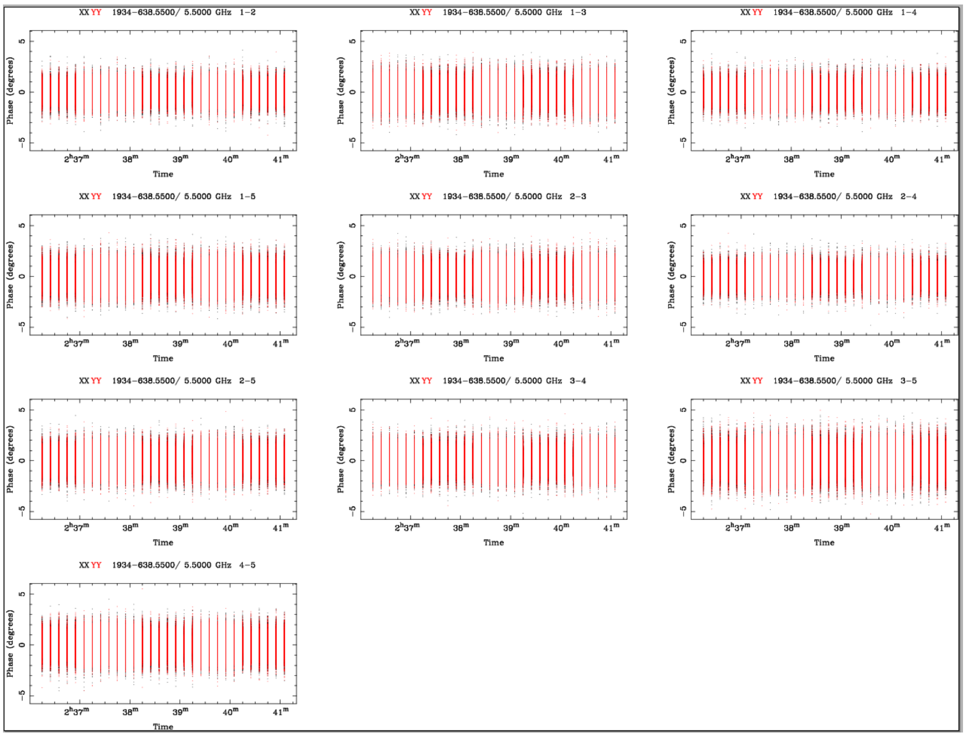

Figure 2.7: phase *vs* time for XX YY correlations

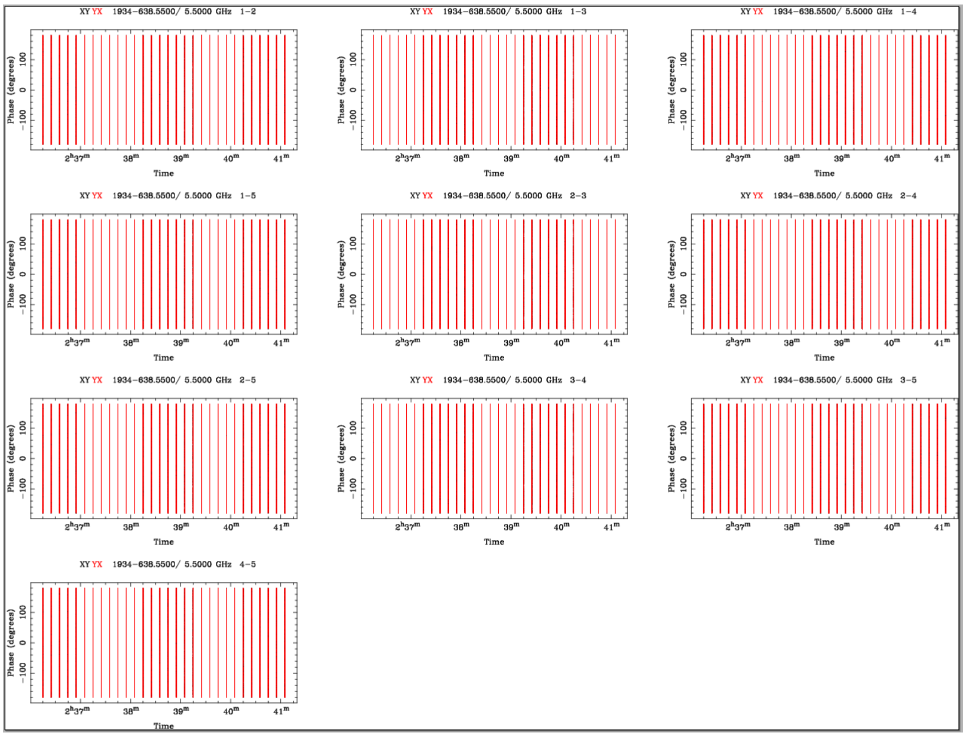

Figure 2.8: phase *vs* time for XY YX correlations

Another way to check the calibration quality is an imaginary amplitude *vs* real amplitude plot. For a source with little flux variation over the bandwidth, Im(amp) *vs* Re(amp) plot should appear as a circle centred on an imaginary value of 0 Jy and a real value of the flux of the source but for a source with varying flux across the bandwidth we see a dumbbell or cigar shape. If radius of circular portion is more than 1 or 2 units then source requires further flagging. Fig 2.9 depicts the imaginary vs real plot for calibrated 1934-638 for parallel and orthogonal correlations and from the figure its clear that it do not requires any further flagging.

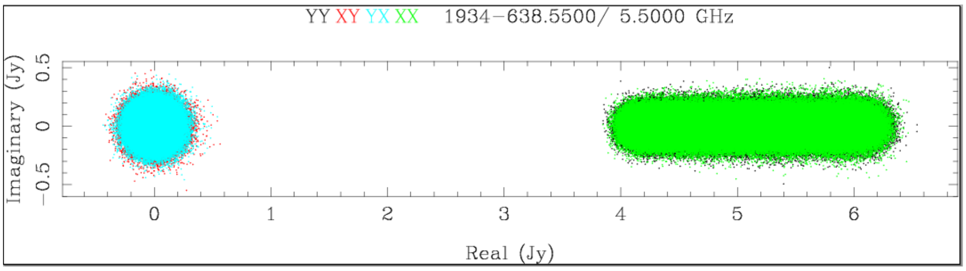

Figure 2.9: real and imaginary amplitudes of the calibrated visibilities for 1934-638

Now at this point, the bandpass and flux calibration for 1934-638 is complete and we proceed now to phase calibrator 2353-686. We perform calibration on 2353-686 by copying the calibration solutions from 1934-638 onto it through task *gpcopy*.

miriad% inp gpcopy

Task: gpcopy

vis	= 1934-638.5500
out	= 2353-686.5500
mode	=
options	=

and then we plot amplitude *vs* channel for 2353-686 to check for any RFI to be flagged and clearly from Fig 2.10 we see that there is no significant RFI to flag.

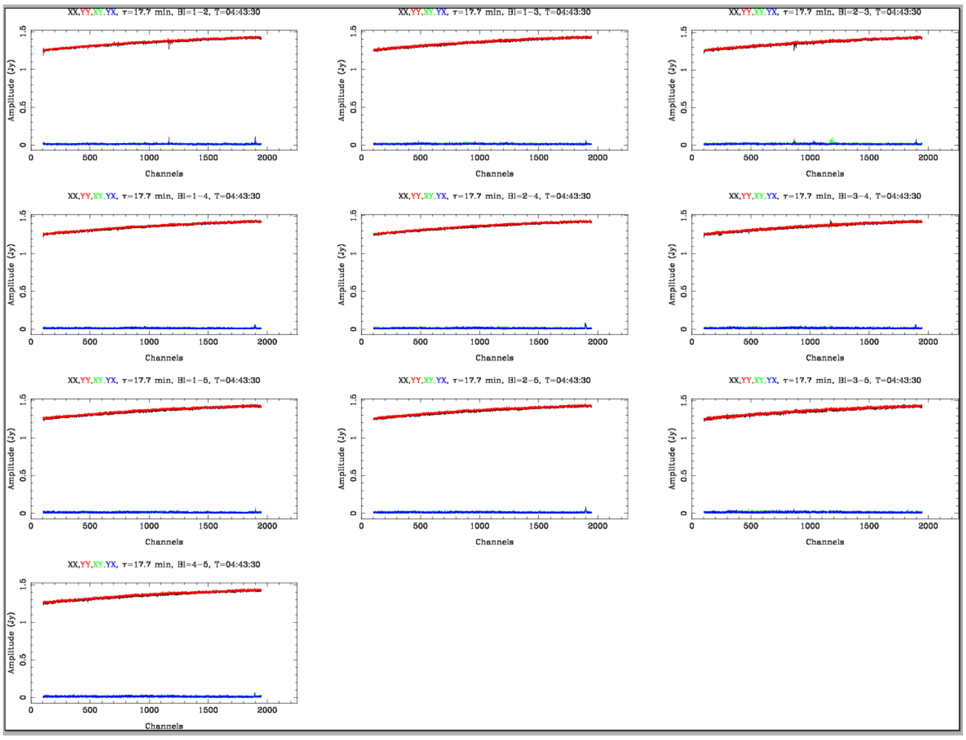

Figure 2.10: amplitude vs channel after copying calibration solutions onto 2353-686

Now we perform task *gpcal* on our phase calibrator. To get an idea of how the gains changed during the observation, we use phase calibrator and to calibrate its gains we use task *gpcal* in the same way as we did for primary calibrator.

```
miriad% inp gpcal
  Task: gpcal
  vis        = 2353-686.5500
  select     =
  line       =
  flux       =
  spec       =
  refant     =
  minants    =
  interval   = 0.1
  nfbin      = 4
  tol        =
  xyphase    =
  options    = xyvary,qusolve
```

As the phase calibrator had enough parallactic angle coverage, option *quslove* was used along with *xyvary* in the above task *gpcal* to get some accurate polarisation measurements.

Again the quality of calibration done on it can be checked by Im(amp) vs Re(amp) plot Fig 2.11.

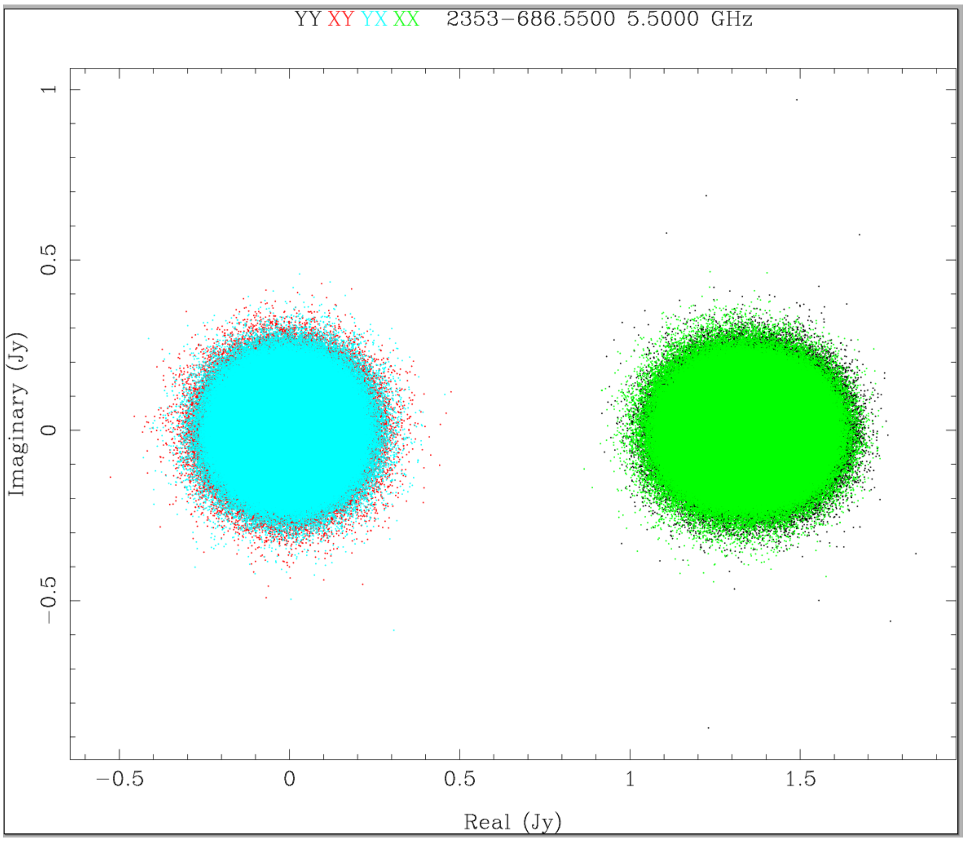

Figure 2.11: Im(amp) vs Re(amp) after phase calibration

Use of task *gpcal* on 2353-686 changes its flux scaling from its true value to slightly different value which differs by a small constant factor and to fix this scaling we use task *gpboot*. It takes the in put as *cal* which has correct flux scaling and uses it onto the visibility (*vis*) which needs to be corrected.

```
miriad% inp gpboot
  Task: gpboot
  vis              = 2353-686.5500
  cal              = 1934-638.5500
  select           =
```

By what factor secondary calibrator got scaled will be displayed on *miriad* prompt. It will display the scaling factor for entire set as well as the individual bins and in our case it was 0.997. Now at this stage calibration and RFI flagging of the calibrators is complete.

2.2.4 Applying Calibration

We first calibrated primary calibrator and using that we calibrated secondary calibrator and now we have to copy the calibration solutions obtained from secondary calibrator to the main source. But before copying the solutions we need to take an average gain solution from the secondary calibrator as the noise on average points will be lower compared to single points. To average gain solutions over time we use task *gpaver*

```
miriad% inp gpaver
  Task: gpaver
  vis            = 2353-686.5500
  interval       = 5
  options        =
```

Everytime 2353-686 was observed, it was done for ≈ 3 minutes so we took *interval* = 5 minutes as we do not want to miss any flux in averaging. After this again one can plot amplitude vs channel and check for any significant RFIs in 2353-686 and can remove them using any of the above mentioned flagging tasks but as we didn't have any RFI in our calibrated visibilities of 2353-686, we proceeded towards copying the calibration to main source using *gpcopy*. Input *vis* is the secondary calibrator from which solutions has to be copied to the main source *rg.5500* given by the input *out*.

```
miriad% inp gpcopy
  Task: gpcopy
  vis            = 2353-686.5500
  out            = rg.5500
  mode           =
  options        =
```

I then used task *uvaver* to convert the *xx,yy,xy,yx* polarization of source *rg.5500* to the stokes parameters - *i,q,u,v* and created a modified output *rg.uvaver.5500* on which further analysis will be carried out.

```
miriad% inp uvaver
  Task: uvaver
  vis          = rg.5500
  select       =
  line         =
  ref          =
  stokes       = i,q,u,v
  interval     =
  options      =
  out          = rg.uvaver.5500
```

We now have a calibrated source *rg.uvaver.5500* which has to go through data reduction on CASA as it will be uncomfortable and time-taking to analyse all the 27 pointings individually on MIRIAD, hence we need to convert the MIRIAD readable *rg.uvaver.5500* to CASA readable format (MS file). We do it by converting it first to a FITS file format using task *fits* on MIRIAD and then converting this FITS file to MS file using task *importuvfits* on CASA.

```
miriad% inp fits
  Task: fits
  in         = rg.uvaver.5500
  op         = uvout
  out        = rg.uvaver.5500.fits
  line       = channel,2049
  region     =
  select     =
  stokes     =
  options    =
  velocity   =
```

uvout - it is used to convert a MIRIAD uv file to FITS uv file.

line - it is used here to specify the number of channels in the output file.

2.3 CASA Analysis

CASA is a next generation data analysis package developed by NRAO to carry out analysis of data which were obtained using wide-band observation over multiple frequencies and which involves mosaicing. To perform data analysis on CASA we need to first convert our data-sets into CASA readable MS format which is done by task *importuvfits* as follows :

CASA <1>: inp importuvfits

———> inp()

fitsfile	= 'rg.uvaver.5500.fits'
vis	= 'rg.uvaver.5500.ms'
antnamescheme	= 'old'
async	= False

Now we have the required data-set *rg.uvaver.5500.ms* which will go through Reduction, Imaging and Deconvolution on CASA.

2.3.1 Data Reduction

Data reduction consists of identifying and removing of RFI from the target source. RFI can be external as well as internal. Interfering satellites and terrestrial telecommunication systems are external RFIs and the electromagnetic devices associated with the telescope are the source of internal RFIs. We used an interactive package *plotms* in CASA for plotting and flagging details of which can be found in CASA cookbook[10]. Fig 2.12 depicts the amplitude vs frequency plot of the calibrated source *rg.uvaver.5500.ms* .

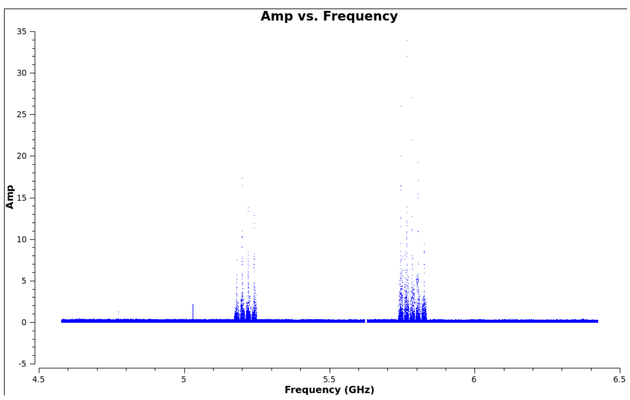

Figure 2.12: amplitude vs frequency plot of rg.uvaver.5500.ms

In the previous plot (2.12) we can clearly see the RFI but there can be chances that not all the 27 pointings would have been affected by same amount of RFI, hence we will remove RFI one by one from individual poinitings. Also from ATNF website we can get the list of identified external RFI[7] and internal RFI[8] which affects the ATCA observation. I removed the external and internal RFI which was mentioned on website. I also observed that after every 3.6 minutes on the amplitude *vs* time plot, there was a similar pattern in the data and considering them as RFI coming from the systematics I removed those data too and then I proceeded towards flagging of the obvious RFI that can be seen in Fig 2.12, one by one from all the pointings. Fig 2.13 and Fig 2.14 depicts the data-set after the removal of all the RFI.

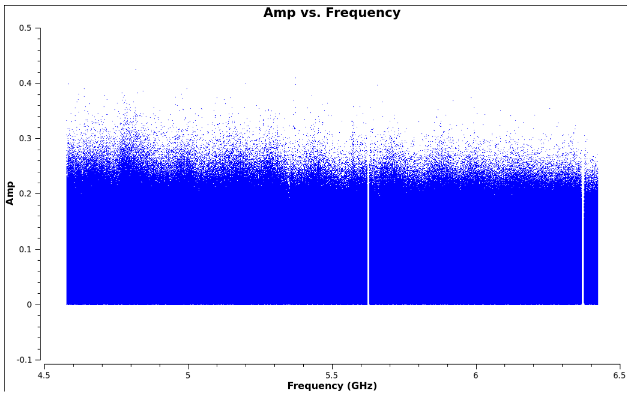

Figure 2.13: amplitude vs frequency plot of rg.uvaver.5500.ms after all RFI removed

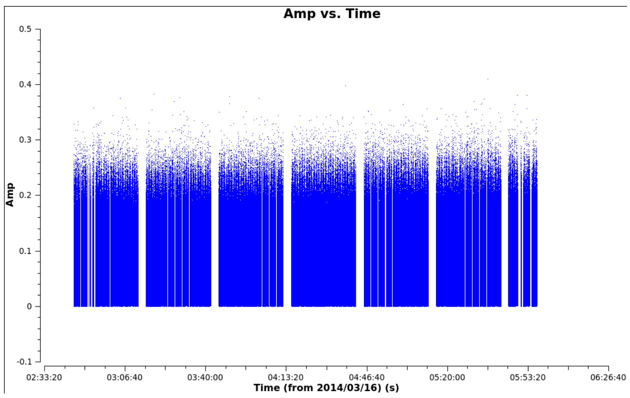

Figure 2.14: amplitude vs time plot of rg.uvaver.5500.ms after all RFI removed

The final *rg.uvaver.5500.ms* obtained after above procedures is calibrated and RFI free and it can be used now for further processing tasks like Imaging and Deconvolution.

2.3.2 Imaging and Deconvolution

As the source was observed over a wide band at two different frequencies and also at 27 different pointings all together making a mosaic, it was beyond MIRIAD's capacity to do the multi-frequency synthesis imaging. Hence we had to shift to CASA for performing Imaging and Deconvolution tasks which is done altogether by a single task *clean*. Imaging involves the Fourier Transformation (FT) of observed visibility thus creating a dirty image of the source and Deconvolution involves recovering a true image of the source from the dirty image by deconvolving the dirty beam from the dirty image. This process can be explained mathematically as follows:

Since dirty image $(I_{DI}(l, m))$[2] is FT of observed visibility $(V_{obs}(u, v))$[3] which is the product of sampling function $(S(u, v))$ and true visibility $(V_{true}(u, v))$, it can be written as

$$\begin{aligned} I_{DI}(l, m) &= FT[V_{obs}(u, v)] \\ I_{DI}(l, m) &= FT[S(u, v).V_{true}(u, v)] \end{aligned} \tag{2.1}$$

Using convolution theorem[9] eqn. 2.1 can be written as :

$$I_{DI}(l, m) = FT[S(u, v)] * FT[V_{true}(u, v)] \tag{2.2}$$

Now the FT of sampling function gives the dirty beam $(I_{DB}(l, m))$ also called as Point-Spread Function (PSF), and FT of true visibility $(V_{true}(u, v))$ gives us the true image $(I_{true}(l, m))$. Hence eqn. 2.2 can be written as :

$$I_{DI}(l, m) = I_{DI}(l, m) * I_{true}(l, m) \tag{2.3}$$

As we can see in eqn. 2.3 dirty image is a convolution of dirty beam and true image, it requires deconvolution of dirty beam from the dirty image to recover the true image and that is done by task *clean*.

After running task *clean* on *rg.uvaver.5500.ms* and *rg.uvaver.9000.ms* for single iteration we got the cleaned image of our galaxy at 5.5GHz and 9GHz which is shown in Fig 2.15.

---

[2] l,m are coordinates in the tangent plane of the sky

[3] u,v are the two components of baseline vector

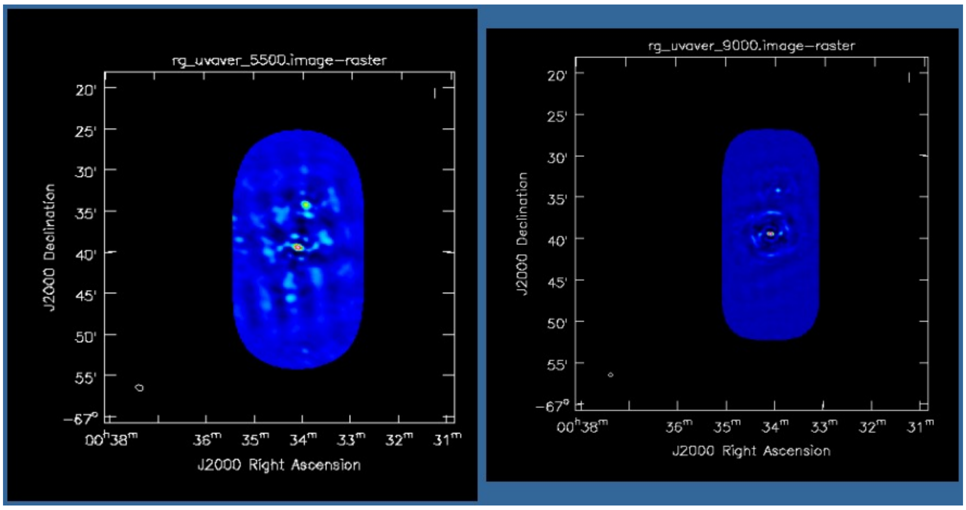

Figure 2.15: True map of target source at 5.5GHz (L) and 9GHz (R) after single iteration of *clean*

We now concatenated the 5.5GHz and 9GHz data in a single data-set *rg.concat.ms* using the task *concat* in CASA and ran *clean* on it for single iteration to get Fig 2.16. Also in Fig 2.17 I have shown a comparison between this concatenated image and the earlier 1.4 GHz image of our target source. I have related the inner northern hotspots and possible southern hotspots which can be due to the restarted activity at the central AGN.

```
CASA <2>: inp concat
———> inp()
vis = [‘rg.uvaver.5500.ms’, ‘rg.uvaver.9000.ms’]
concatvis = ‘rg.concat.ms’
freqtol = ‘ ’
dirtol = ‘ ’
respectname = False
timesort = False
copypointing = True
visweightscale = [ ]
```

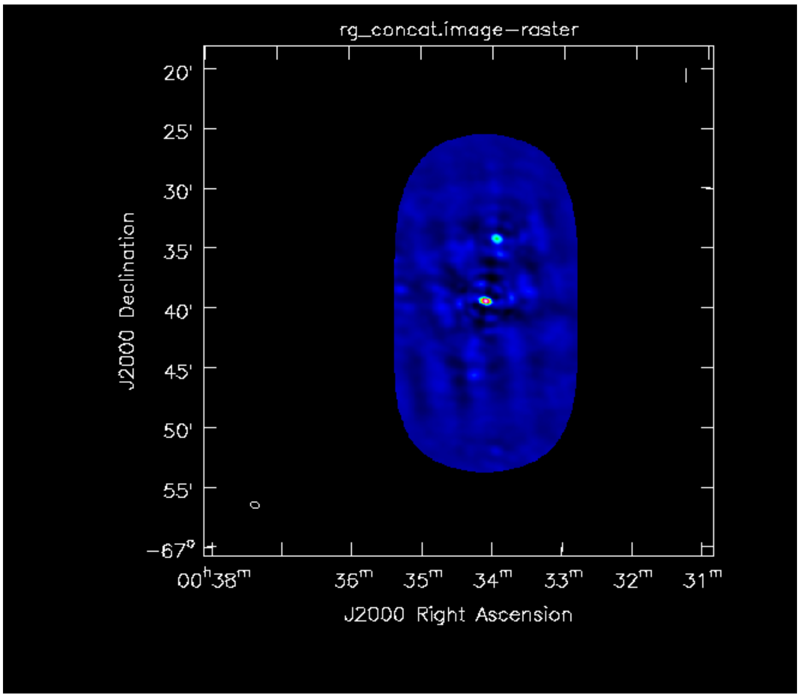

Figure 2.16: True map of source after single iteration of *clean*

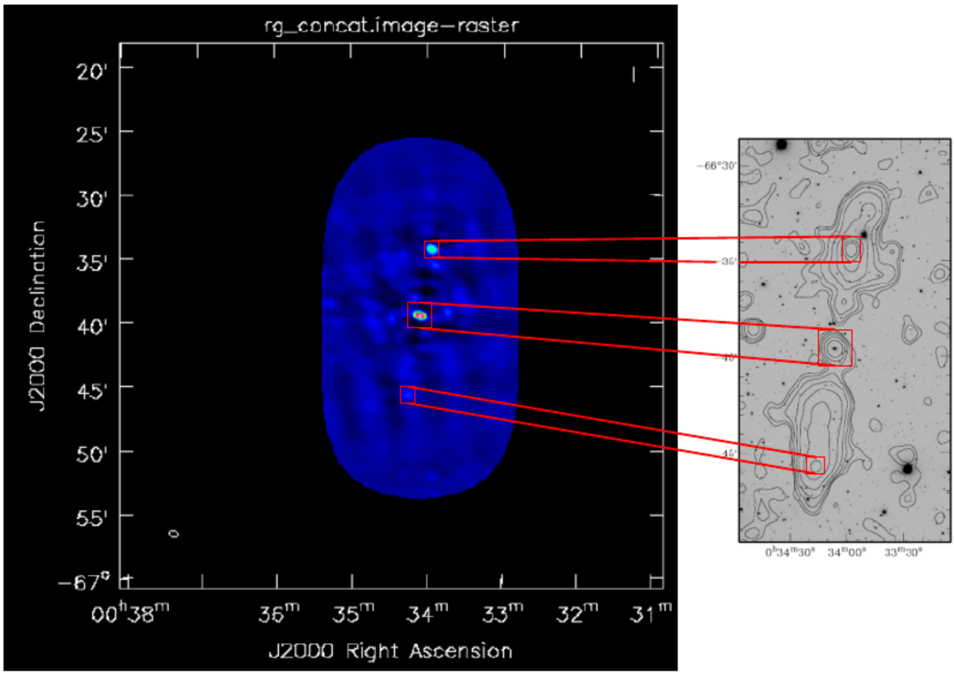

Figure 2.17: Comparison between the concatenated image and 1.4 GHz image

From the above Fig 2.16 it is depicted that image of the radio galaxy is not clear and there are loads of artefacts still present in the data, hence it requires further more cleaning[4].

[4]Parameters of task *clean* is discussed in appendix

A | Task *Clean*

Following are the parameters used in task *clean* on the concatenated data *rg.concat.ms* details about which can be found in CASA cookbook[10].

CASA <3>: inp importuvfits
——> inp()
vis = 'rg.concat.ms' ; Name of input visibility file
imagename = 'rg_concat' ; Pre-name of output images
outlierfile = ' '
field = ' '
spw = ' '
selectdata = False ; Other data selection parameters
mode = 'mfs' ; Spectral gridding type (mfs, channel, velocity, frequency)
nterms = 1 ; Number of Taylor coefficients to model the sky frequency dependence
reffreq = ' '
gridmode = ' '
niter = 1 ; Maximum number of iterations
gain = 0.01 ; Loop gain for cleaning
threshold = '0.0mJy' ; Flux level to stop cleaning, must include units: '1.0mJy'
psfmode = 'clark' ; Method of PSF calculation to use during minor cycles
imagermode = 'mosaic' ; Options: 'csclean' or 'mosaic', '', uses psfmode
mosweight = False
ftmachine = 'mosaic'
scaletype = 'SAULT'
cyclefactor = 1.5
cyclespeedup = -1
flatnoise = True

multiscale = [ ]
interactive = False
mask = [ ]
imsize = [512, 512] ; x and y image size in pixels. Single value: same for both
cell = ['5.0arcsec'] ; x and y cell size(s). Default unit arcsec.
phasecenter = ['J2000 00h34m28 -66d39m32'] ; Image center: direction or field index
restfreq = ' '
stokes = 'I' ; Stokes parameters to image (eg. I,IV,IQ,IQUV)
weighting = 'natural' ; Weighting of uv (natural, uniform, briggs, ...)
uvtaper = False
modelimage = ' '
restoringbeam = [' ']
pbcor = False
minpb = 0.2
usescratch = False
allowchunk = False
async = False

Clean task works on an algorithm which involves following steps :

1) Assumes the dirty image as a collection of point sources
2) Finds the highest peak in it
3) Subtracts out some percentage of this peak (gain factor) using scaled dirty beam (psf) (*rg_concat.psf*)
4) Adds the subtracted amplitude in a clean component list
5) Goes to step 2 unless a mentioned threshold or iterations is reached
6) Adds back the clean components convolved with a clean beam to the residual map (*rg_concat.residual*) and the resulting image (*rg_concat.image*) thus obtained is the true image of the source.

It took ~2.5 hours in execution of *clean* resulting in following 6 outputs :
rg_concat.image - it's the true image of the source
rg_concat.flux - it's the effective response (primary beam) of the telescope
rg_concat.flux.pbcoverage - it's the effective response of the full mosaic image
rg_concat.model - it contains all the clean components
rg_concat.psf - it's the dirty beam
rg_concat.residual - it shows what is left at the end of deconvolution process and is useful to decide whether further cleaning is required or not.

Bibliography

[1] ATLBS

[2] L. Saripalli et al. 2012 ApJS 199 27

[3] ATCA

[4] Sault, R. J., Teuben, P. J., & Wright, M. C. H. 1995, Astronomical Data Analysis Software and Systems IV, 77, 433

[5] http://casa.nrao.edu/

[6] MIRIAD Cookbook

[7] http://www.narrabri.atnf.csiro.au/operations/rfi/rfi_ext.html

[8] http://www.narrabri.atnf.csiro.au/operations/rfi/rfi_int.html

[9] Convolution Theorem

[10] CASA Cookbook